Effect of Geometric Differences Impeller Blades on Performance Blower-as-Turbine (BAT) on Pico-Hydro Scale

Asep Neris Bachtiar*‡, Ahmad Fauzi Pohan**, Riko Ervil***, Nofriadiman****, Santosa*****, Isril Berd*****, Uyung Gatot S. Dinata******

*Department of Mining Engineering, Industrial Technology High School of Padang, Jl. Prof. Dr. Hamka No. 121, Padang, 25171, Indonesia.

** Department of Physics, Faculty of Mathematical and Science, Andalas University, Jl. Universitas Andalas Limau Manis Pauh, Padang, 25163, Indonesia.

*** Department of Industrial Engineering, Industrial Technology High School of Padang, Jl. Prof. Dr. Hamka No. 121, Padang, 25171, Indonesia

****Department of Information Systems , Industrial Technology High School of Padang, Jl. Prof. Dr. Hamka No. 121, Padang, 25171, Indonesia

***** Department of Agriculture Engineering, Faculty of Agricultural Technology, Andalas University, Jl. Universitas Andalas Limau Manis Pauh, Padang, 25163, Indonesia.

****** Department of Mechanical Engineering, Faculty of Engineering, Andalas University, Jl. Universitas Andalas Limau Manis Pauh, Padang, 25163, Indonesia.

(asepnerisb@sttind.ac.id, ahmadfauzipohan@sci.unand.ac.id, rikopdg01@gmail.com, nofriadiman@sttiind.ac.id, santosa@fateta.unand.ac.id, isberd@yahoo.com, uyunggsd@ft.unand.ac.id)

‡Corresponding Author; Asep Neris Bachtiar, Jl. Prof. Dr. Hamka No. 121, Padang, 25171, Indonesia,

Tel: +62 813 7423 1006, asepnerisb@sttind.ac.id

Received: 05.04.2021 Accepted:07.05.2021

Abstract- The classification of centrifugal blowers is determined by the geometry of the angle when water leaves the outer side of the impeller blade (β), namely $\beta > 90^0$, $\beta = 90^0$, and $\beta < 90^0$. If the blower is used as a turbine (BAT), then the blower with an angle $\beta > 90^0$ has characteristics which is relatively the same as the Francis turbine impeller blades, but the blower type $\beta > 90^0$ is rarely sold in the market, which is widely sold in the market is the blower with angle $\beta < 90^0$. The performance of BAT $\beta < 90^0$ can be improved by changing or modifying the geometry of the angle β to BAT $\beta = 90^0$ and BAT $\beta > 90^0$. The aim of this study was to analyze the performance of BAT $\beta = 90^0$ and BAT $\beta > 90^0$ and compare them with the original BAT ($\beta < 90^0$). The research method is an experiment, the results of testing and analysis prove that differences in the geometry of BAT impeller blades have an effect on BAT performance. The results showed that the efficiency of BAT $\beta > 90^0$ was better than the efficiency of the straight BAT blade (BAT $\beta = 90^0$) and the original BAT blade (BAT $\beta < 90^0$), namely 69.42 % compared to 59.10 % and 50.90 %. The starting discharge ratio is getting smaller, namely 0.22 compared to 0.27 and 0.30. This shows that BAT $\beta > 90^0$ is more responsive in generating power.

Keywords : Centrifugal blowers, impeller, blower-as-turbine, BAT, pico-hydro.

1. Introduction

The energy needs of the world community are increasing indefinitely. The development of energy systems through the exploitation of various natural resources such as petroleum and coal has been carried out in recent years, this phenomenon has led to an increase in harmful pollutants in the atmosphere [1]. The importance of renewable energy sources is a concern today because of the limitations of energy sources that are not renewable and not environmentally friendly [2]. The use of renewable energy systems is the best alternative to achieve a reduction in the high cost of energy supply and carbon emissions arising from the use of fossil fuels [3]. Renewable energy production requires serious attention in developing countries, the choice of an effective renewable energy technology that is economically feasible and environmentally acceptable is an interesting topic due to the availability of various types of renewable energy sources. Proper investigation and research is needed to determine the ideal renewable energy technology [4]. Renewable energy innovation and development has increased rapidly in recent years [5]. Many solutions have been tried to solve people's energy needs, but the problem of availability and quality of renewable energy has not been maximized so that it becomes a challenge especially felt by people in villages [6]. The energy needs of the villagers must be met with a reliable, uninterrupted supply of energy. The development of the rural energy sector through the integration of renewable energy systems will in turn pave the way to meet the increasing demand for electricity. This can be done through a better understanding of renewable energy system integration [2]. In the power generation system, the reliable and efficient performance of the generating unit to meet the demands of demand is of great importance [7]. The implementation of maintenance that is disciplined, timely, and appropriate in its utilization has a major impact on service quality and efficiency of generating costs [8].

There are many renewable energy sources that can be used to obtain electrical energy from natural sources in the world. The most widely known renewable energy sources are solar, wind, and hydro energy [9]. Indonesia is an archipelagic country that has great potential for water energy resources including tidal currents and wave power [10]. Hydropower plants at micro and pico-hydro scale have proven to play an important role in fulfilling renewable energy for society. One of the challenges is that water turbines are not sold freely in the market. To get them, people have to order in advance so that the turbine price becomes expensive [11]. Conventional turbines used for small-scale hydroelectric power plants (pico-hydro and micro-hydro) include cross flow turbines, Francis turbines, pelton turbines, and propeller turbines. The use of cross flow turbines is relatively more practical in a pico hydro generating system that is capable of producing 8.9 kW of power with an optimal efficiency of up to 89 % [12].

Energy security is a complex and multi-dimensional research field. There are five dimensions commonly used by researchers, namely availability, affordability, technology-efficiency, governance-regulation and environment sustainability. Research to improve plant performance has been carried out by researchers by modifying turbine runners so that turbine efficiency can be increased. [13] Efforts to improve the performance of pico-hydro plants were carried out using cross flow turbines and it is known that water velocity has a positive effect on the performance of pico-hydro plants. Numerical studies have been carried out to improve the efficiency of the Michell Banki turbine or cross flow turbine by modifying one of its geometric parameters, namely the profile of the runner blades. The simulation results show an increase in efficiency of 7.37 %, 7 % and 0.76 % respectively with blade profiles of 20-32C, NACA 9412-ST and NACA 9412-15 [14]. Furthermore the Archimedes screw turbine is being explored worldwide as one of the best candidates for efficient pico-hydro power generation in locations with low head and low flow rates. Experimental analysis shows that an approx. Thread angle below 25^0 and a flow rate below 1.5 L/s can increase the efficiency of the Archimedes screw turbine to about 90 % as long as the rotation speed is kept at an optimal level to reduce losses in the turbine [15]. Several studies have successfully tested the performance of a fluid engine that is converted into a water turbine, the research results prove that pumps, compressors, and blowers can be used as alternative water turbines. The test results of three pump-units-as-turbines (PAT) with the same installation at a constant head, it is known that the smaller pump size produces greater head, torque, power and efficiency. 1 inch PAT is superior to 1.5 inch PAT, and 2 inch PAT. These data inspired the investigators to create a head and discharge standard suitable for each PAT measure [16].

Other studies have successfully tested the performance of the compressor-as-turbine (CAT), the centrifugal compressor that was tested came from a turbo charger component. The test results at a constant head of 4.7 m and four variations of valve openings, it is known that the greater the valve opening can result in better torque, power, efficiency and rotation speed. At 100 % valve opening with a water discharge of 14.0 L/s, it results in a maximum torque performance of 10.70 N m, a maximum turbine power of 342.11 W and a maximum efficiency of 52.74 % [17]. Furthermore, the laboratory test results with the same test installation on four sizes of centrifugal blowers-as-turbines (BAT) are as shown in Fig. 1 [18] without changing the impeller blade geometry. It is known that the smaller the blower size results in better efficiency performance. The 2-inch BAT delivers higher efficiency than the 2.5-inch, 3-inch, and 4-inch BATs. The 2-inch BAT performance is capable of producing 8.30 N m of torque, 583 W of power, and a maximum efficiency of 50.90 % which occurs at a constant head of 14 m, a discharge of 8.34 L/s, and a rotational speed of 800 rpm. Another BAT test at a constant rotational speed of 800 rpm and a discharge ratio of 0.9 to 1.0 resulted in a slightly decreased trend in efficiency. This finding explains that BAT is starting to become saturated or less sensitive to changes in discharge ratios above 0.9. This is due to the impeller construction that can not keep up with or adjust to the addition of water discharge. BAT performance can be improved by making modifications to the BAT impeller blade to resemble a Francis turbine impeller blade with a geometry that challenges the direction of water entering the blade [24].

Fig. 1. Centrifugal blowers of size 4-inch, 3-inch, 2.5-inch, and 2-inch not modified ($\beta < 90^0$)

Subsequent literature studies have succeeded in summarizing the similarities and differences in the characteristics of the blower, Francis turbine and original BAT as shown in Fig. 2 [19]. The similarity between the three is having the same volute. The Francis turbines and BAT have the same direction of flow of water into the impeller. The analysis of the speed triangle on the blower and BAT is relatively the same, what distinguishes between the two is the direction of water velocity when leaving the impeller or towards the impeller. Another interesting thing about centripugal blowers is that it is theoretically known that there are three types of centrifugal blower impellers. The difference between the three is determined by the geometry of the angle when water leaves the outer side of the impeller blade (β), namely $\beta > 90^0$, $\beta = 90^0$, and $\beta < 90^0$ as shown in Fig. 3 [20]. The types of blowers that are sold in the market are blower types with angles $\beta < 90^0$. If it functions as a turbine, it turns out that the blower with blade geometry $\beta < 90^0$ has different characteristics from the blades of a Francis turbine impeller. The geometry of the impeller blade with angle $\beta < 90^0$ is behind the direction of water entering the blade while the geometry of the Francis turbine impeller blade challenges the direction of water entering the blade. The similarity of BAT $\beta < 90^0$ with the Francis turbine is that they both have the same volute housing construction. The results of this analysis confirm the researcher's hypothesis that the performance of BAT $\beta < 90^0$ can be improved by making changes or modifications to the blade. geometry of the impeller blades, namely by fixing the curvature of the impeller blades to resemble the curvature of the Francis turbine impeller blades. This study will test the performance of the modified BAT, namely the straight blade BAT ($\beta = 90^0$) and the BAT blade challenging ($\beta > 90^0$) and compare it with the performance of the original BAT, namely the backward blade BAT ($\beta < 90^0$).

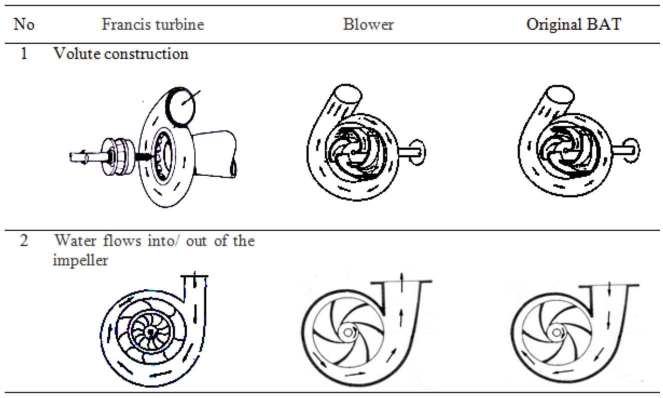

Fig 2. Comparison of the characteristics of the Francis turbine, blower, and original BAT

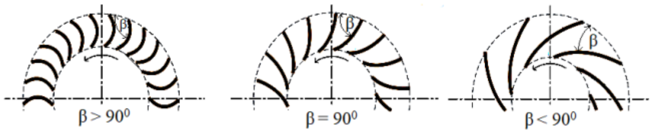

Fig. 3. Three types of centrifugal blower impeller

2. Research Methodology

The research stage begins with modifying the blower, preparing the installation of testing equipment, procuring materials and measuring instruments, assembling and installing it, the testing phase, and analyzing the test data. The preparatory stage is checking the installation of leaks and checking the performance of the pump as a source of discharge and head. The material procurement stage is the procurement of three 2-inch centrifugal blowers and the procurement of rotational speed measuring instruments and torque measuring instruments. There was no modification for one blower (original BAT : $\beta < 90^0$) but for two more blowers the blade geometry was modified ($\beta > 90^0$, $\beta = 90^0$). The next stage is the installation of BAT in installation, testing and analysis. Tests carried out on four variations of constant head, in each head there are ten variations of rotation speed and discharge. The test result variables are BAT rotation speed (N), BAT toque (T_b) discharge (Q), BAT efficiency (η_b), BAT power (P_b), and potential power (P_p).

2.1 Test Location

The test installation is shown in Fig. 4 [21] with the main components being a reservoir, piping and pump as a source of discharge and pressure or head. The test location is at the Fluid Dynamics Laboratory, Department of Mechanical Engineering, Andalas University, Fig. 5 shows the BAT when it is installed in the testing installation.

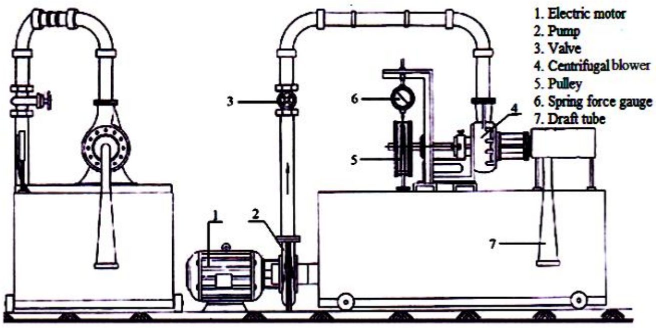

Fig. 4. BAT three-type test installation

Fig. 5. BAT installed in the test installation

2.2. Modification Stage

Changing the function of the blower to a turbine requires modification, namely removing half of the motor cover so that the motor and bearings at the end of the blower shaft are easily seen. The stator of the electric motor attached to the blower shaft is removed to facilitate the installation of the 3 inch pulley as shown in Fig. 6. The 3 inch pulley serves as a complete measurement of the torque that occurs when the blower functions as turbine.

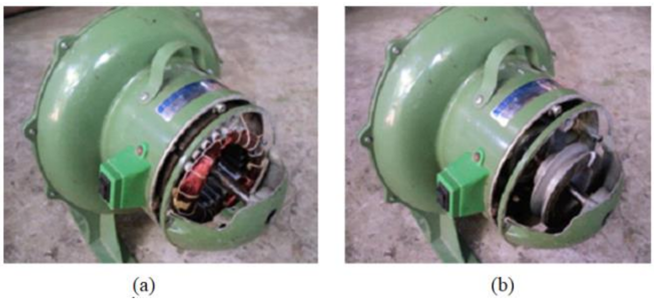

Fig. 6. Close the blower split, visible motor stator (a), the stator is removed and replaced with a 3-inch pulley (b)

The next modification action is to improve the geometry of the blower impeller blades to resemble the geometry of the Francis turbine impeller blades. The geometry of the BAT impeller blade before modification is backward to the direction of water entering the impeller or the angle of water entering the blade is smaller than 90^0 ($\beta < 90^0$). The measurement results show that the water angle into the original BAT blade is 74^0 or 16^0 less than 90^0. After being modified through the heating and pressing process, two variations of blade geometry are produced, namely BAT straight blade geometry or no curved blade ($\beta = 90^0$) and BAT with blade geometry challenging the direction of water entering the impeller with the angle of water entering the blade $\beta > 90^0$, namely $\beta = 90^0 + 16^0 = 106^0$. This research has successfully tested the performance of three types of BAT, namely BAT $\beta > 90^0$, BAT $\beta = 90^0$, and BAT $\beta < 90^0$ or the original BAT as shown in Fig. 7.

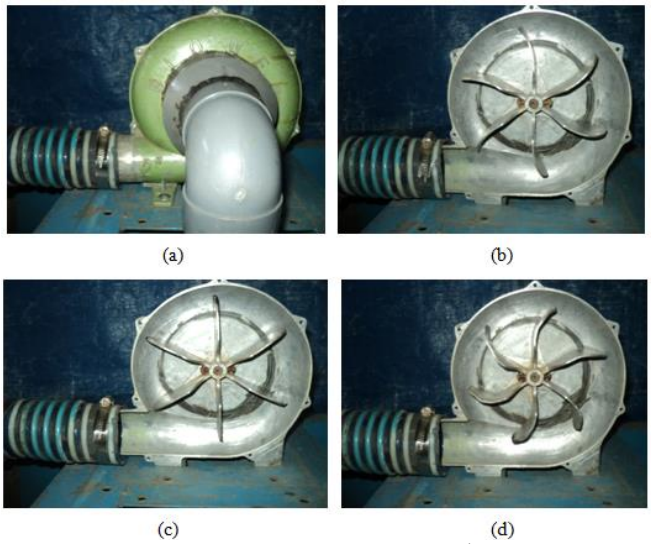

Fig. 7. BAT when tested (a), BAT $\beta < 90^0$ or original BAT (b), BAT $\beta = 90^0$ (c), and BAT $\beta > 90^0$ (d)

The next modification stage is to install the draft tube in the outlet hole in the form of a PVC elbow. The inlet pipe is selected from spiral pipe material which is flexible enough to facilitate installation and locking. In the BAT system, the blower inlet and outlet holes change into an outlet hole and an inlet hole. The BAT system when installed in the test installation is shown in Fig. 8.

Fig. 8. Position of the inlet pipe and outlet pipe (draft tube)

2.3. Constant Head Analysis

Performance testing of three types of BAT was carried out with four constant head variations. The constant head can be determined by adjusting the valve opening to the desired pressure position. The constant head is known from the pressure on the pressure gauge installed at the end of the inlet pipe as shown in Fig. 9. The pressure gauge used has a maximum pressure scale of 2.5 atm which is proportional to a 25 m head or theoretically it is stated that 1 atm is equal to a 10 m head of water [22].

Fig. 9. A pressure gauge is installed at the end of the inlet pipe

2.4. Technical Data Analysis

The next step after the modification, assembly and installation of BAT components is the BAT performance test. In each impeller and constant head model, measurements of BAT torque (T_b), BAT rotation speed (N), potential power (P_p), BAT power (P_b), and BAT efficiency (η_b) were measured. The measurement of the BAT rotational speed uses a digital tachometer that is fixed at the end of the shaft and the measurement of the torque is carried out by braking the rotational speed of the pulley attached to the end of the BAT shaft. The BAT torque measurement scheme is described in Fig. 10. The test equipment used consisted of bands and digital scales. In the braking process, the tension on the tight side (F_t) and the slack side of the band (F_s) will arise, the difference between F_t and F_s is obtained effective force (F_e). The torque that occurs can be searched by equation (1) [29].

$$T_b = F_e \times R \quad (1)$$

Where, R is the pulley radius (R = 1.5 inches)

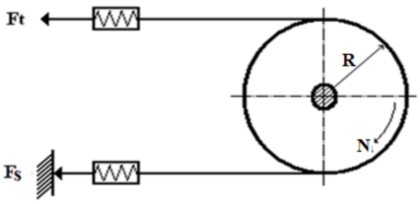

Fig. 10. BAT torque measurement scheme

The BAT power (P_b) and potential power (P_p) can be known from equations (2) [29] and (3) [23]

$$P_b = 6.28 \times N \times T_b / 60 \quad (2)$$

$$P_p = \rho_{water} \times g \times Q \times H \quad (3)$$

ρ_{water} is the dencity of water (1000 kg/m^3). The efficiency of the BAT (η_b) can be seen from equation (4) [24].

$$\eta_b = (P_b / P_p) \times 100\ \% \quad (4)$$

Turbine discharge (Q) is the same as water flowing out through the triangle door which is one of the components of the weirmeter. The variables that deter mine the size of the discharge are the height of the water in the reservoir (h_w) and the width of the triangle door (b = 0.6 m) which are then analyzed by equation (5) [24].

$$Q = c \times h_w^{5/2} \quad (5)$$

c is the coefficient of discharge that can be found by equation (6) [27].

$$c = 81.2 + (0.24/h_w) + \{(43.08\ (h_w/b - 0.09)\}^2 \quad (6)$$

3. Results and Discussion

BAT performance and characteristics tests include how the torque, power, and efficiency trends due to the influence of variations in rotational speed and discharge variations at four constant head variations.

3.1. Effect of Variation of Rotation Speed (N) on Torque of three types of BAT (T_b) at Four Head Constant Variations

The purpose of the test is to determine the trend of the torque curve that occurs due to variations in rotational speed and to determine the maximum torque and optimum rotational speed. The torque data that occurs in each rotation is known from the results of the braking test as shown in Fig. 11 and the analysis is described in equation (1). The data recapitulation of the three BAT types of test results is displayed only at a constant head of 14 m as shown in Tables 1-3, while the recapitulation of test data at a constant head of 4 m, 6 m, and 10 m is not shown due to limitations. Furthermore, the rotational speed data in column 2 and torque data in column 5 are plotted into the curve, then the BAT torque trend is as shown in the curve in Fig. 12 - 14.

Fig. 11. BAT **torque** measurement

Table 1. The test data is BAT β < 90^0 with a constanthead of 14 m

No	Rotational Speed, N (rpm)	Discharge, Q (L/s)	Potential Power, P_p (W)	BAT Torque, T_b (N m)	BAT Power, P_b (W)	BAT Efficiency, η_b (%)
1	0	11.00	1538.21	15.00	0.00	0.0
2	160	10.82	1483.27	13.37	223.97	15.1
3	260	10.61	1455.80	12.20	331.92	22.8
4	380	10.33	1414.60	11.45	455.50	32.2
5	610	9.52	1304.73	9.38	598.87	45.9
6	800	8.34	1145.54	6.96	583.02	50.9
7	970	7.33	1002.58	4.66	473.16	47.2
8	1100	6.71	920.18	3.30	380.58	41.3
9	1210	6.32	865.24	2.42	307.20	35.5
10	1400	5.62	769.10	1.12	164.07	21.3
11	1600	5.00	686.70	0.00	0.00	0.0

Table 2. The test data is BAT $\beta = 90^0$ with a constant head of 14 m

No	Rotational Speed, N (rpm)	Discharge, Q (L/s)	Potential Power, P_p (W)	BAT Torque, T_b (N m)	BAT Power, P_t (W)	BAT Efficiency, η_t (%)
1	0	11.20	1538.21	15.80	0	0
2	180	10.82	1483.27	13.79	259.87	17.52
3	290	10.61	1455.80	12.68	385.06	26.45
4	550	10.33	1414.60	10.25	590.35	50.35
5	690	9.52	1304.73	9.48	684.63	53.24
6	900	8.34	1145.54	7.40	696.87	59.03
7	1250	7.33	1002.58	4.67	610.92	54.75
8	1390	6.71	920.18	3.44	500.43	47.97
9	1580	6.32	865.24	2.12	350.30	35.18
10	1680	5.62	769.10	1.03	180.35	23.45
11	1850	5.00	686.70	0	0	.0

Table 3. The test data is BAT $\beta > 90^0$ with a constant head of 14 m

No	Rotational Speed, N (rpm)	Discharge, Q (L/s)	Potential Power, P_p (W)	BAT Torque, T_b (N m)	BAT Power, P_b (W)	BAT Efficiency, η_b (%)
1	0	11.20	1538.21	17.50	0	0
2	200	10.82	1483.27	16.71	349.91	23.59
3	320	10.61	1455.80	14.17	474.59	32.6
4	470	10.33	1414.60	13.24	651.42	46.5
5	750	9.52	1304.73	10.40	816.42	65.4
6	980	8.34	1145.54	8.19	840.73	72.8
7	1190	7.33	1002.58	6.23	776.64	70.9
8	1350	6.71	920.18	4.84	684.19	64.4
9	1490	6.32	865.24	4.10	639.28	55.7
10	1720	5.62	769.10	1.86	334.65	30.1
11	1970	5.00	686.70	0.00	0	0

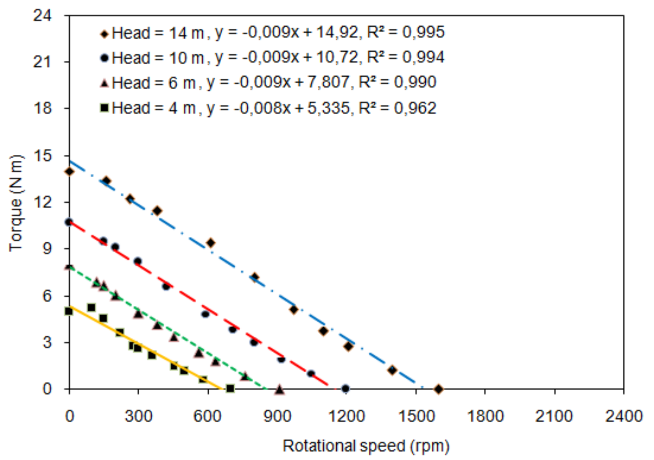

Fig. 12. BAT $\beta < 90^0$ torque curve due to the influence of rotation variations

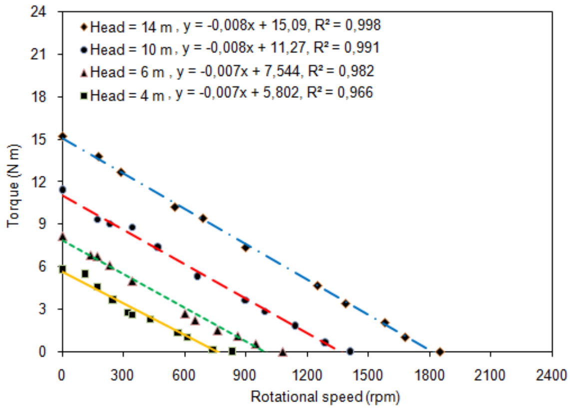

Fig. 13. BAT $\beta = 90^0$ torque curve due to the influence of rotation variations

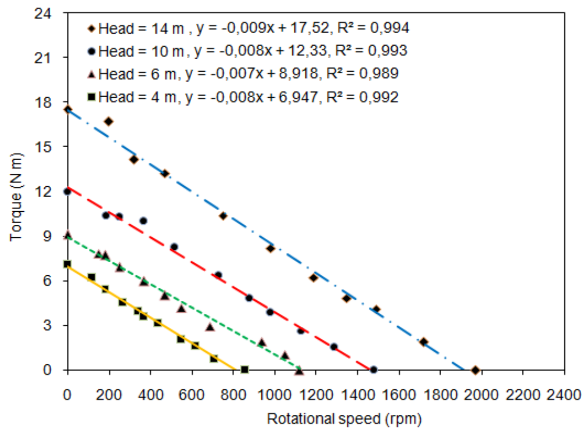

Fig. 14. BAT $\beta > 90^0$ torque curve due to the influence of rotation variations

Fig. 12-14 shows that the three BATs produce a linear torque curve with a downward trend. This shows that the rotational speed (N) has a negative effect on torque (T_b) and there is a regular inverse relationship between the two. BAT with modified blade geometry has a larger curve size. This finding proves the truth of the hypothesis that BAT with impeller blades closer to the shape of the Francis turbine impeller blades will produce better torque and rotational speed. The four curves of each BAT have relatively the same slope, are symmetrical, regular, and do not cross each other. This phenomenon shows that, the three BATs (BAT $\beta > 90^0$, BAT $\beta = 90^0$, and BAT $\beta < 90^0$) can continue to operate stably as a turbine despite variations in rotation speed and constant head. When the braking test is carried out, the effective force (F_e) on the torque tester increases strongly when the turbine is braked until it reaches the lowest rotational speed. On the other hand, in the absence of braking, for example at a high rotational speed of 1500 rpm, the braking force at that time was quite light and continued to change to moderate, strong and very strong according to the decrease in rotational speed until the BAT stopped rotating. The stronger the braking rope force, the greater the operating torque and vice versa. BAT $\beta > 90^0$ has better torque performance than BAT $\beta = 90^0$ and BAT $\beta < 90^0$ (original BAT). At a constant head of 14 m and 11 rotation variation data, it is known that the maximum torque achieved by BAT $\beta > 900$, BAT $\beta = 90^0$, and BAT $\beta < 90^0$ is 17.5 N m, 15.8 N m, and 15 N m, respectively there is a decrease in the average maximum torque about 8.05%. The BAT curve β > 90^0 in Fig. 14 shows that at a constant head of 14 m, 10 m, 6 m, and 4 m, the maximum torque is 17.5 N m, 12 N m, 9.1 N m, and 7.1 N m, respectively the average torque reduction is around 25.84 %.

3.2. The Effect of Variation of Rotation Speed (N) on the Power of three types of BAT (P_b) at Four Constant Head Variations

The purpose of the test is to determine the power curve trend which is formed due to variations in rotational speed and constant head variation of the three types of BAT tested, namely BAT β > 90^0, BAT β = 90^0, and BAT β < 90^0. Other information will be disclosed in each of them. BAT is what is the optimum rotation speed that produces maximum power. After the torque (T_b) data for ten variations in rotational speed are obtained, then the BAT power (P_b) can be immediately known through equation (2) and examples of the analysis results are listed in column 6 Tables 1-3. The resulting BAT power trend curve for four constant head variations is shown in Fig. 15-17.

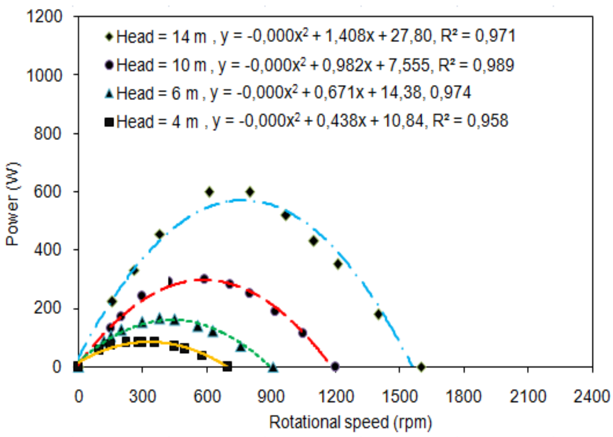

Fig. 15. BAT β < 90^0 power curve due to the influence of rotation variations

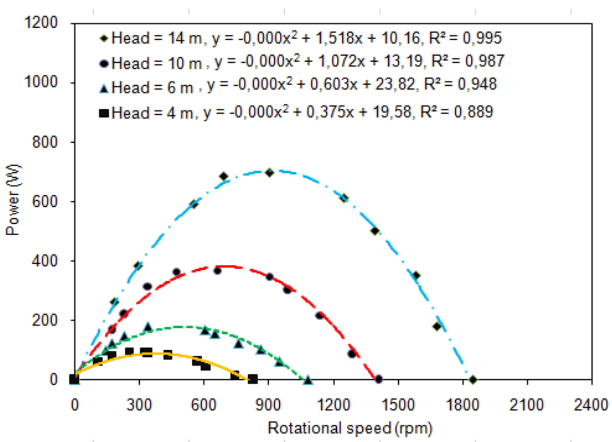

Fig. 16. BAT β = 90^0 power curve due to the influence of rotation variations

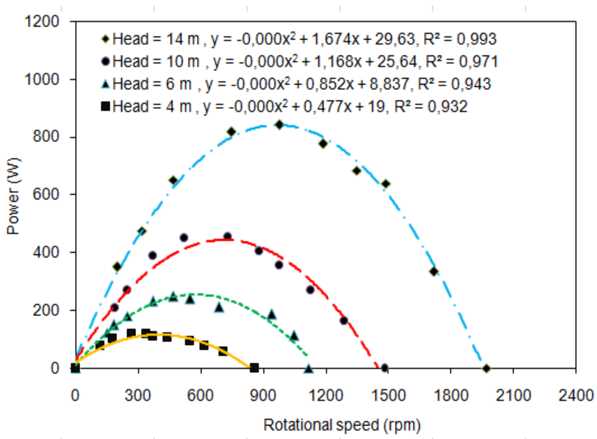

Fig. 17. BAT β > 90^0 power curve due to the influence of rotation variations

Fig. 15-17 shows that the size of the modified BAT impeller power parabolic curve (BAT β > 90^0 and BAT β = 90^0) is larger than the original BAT impeller power parabolic curve (BAT β < 90^0). This shows an increase in performance after the BAT was modified and it is evident that the impeller blades that challenge the direction of water entering the blade produce better performance. The four parabolic curves in each BAT image have relatively the same pattern. The fourth curve covers the third curve, the third curve covers the second curve and the second curve covers the first curve, the difference lies in its size. In the first half of the rotation speed interval, there is an increase in power in accordance with the increase in rotational speed, and in the second rotation speed interval, there is a decrease in power until it reaches the lowest power. This is because at high rotational speeds the BAT has decreased loading due to braking so that the torque and power are low. In each image shown, there is a drastic increase in BAT power at a maximum constant head of 14 m. BAT β > 90^0 produces a maximum power of 840.7 W at a rotational speed of 980 rpm. BAT β = 90^0 produces a maximum power of 696.9 W at a rotational speed of 900 rpm, while BAT β < 90^0 produces a maximum power of 598.9 W at a rotational speed of 610 rpm. The percentage of maximum power drop from BAT β > 90^0 to BAT β < 90^0 (original BAT) is about 15.50 %. Especially for BAT β > 90^0, from Fig. 17 it is known that at a constant head of 14 m, the maximum power is 840.7 W which occurs at a rotational speed of 980 rpm. The next maximum power at a constant head of 10 m is 452.2 W at a rotational speed of 730 rpm. The maximum power at a constant head of 6 m is 247.8 W at a rotational speed of 470 rpm, and at a constant head of 4 m, the maximum power is 117.3 W at a rotational speed of 340 rpm.

3.3. Effect of Variation of Rotation Speed (N) on Efficiency of three BAT types (η_b) for Four Constant Head Variations

This test aims to determine the difference in the trend of efficiency curves of the three types of BAT (BAT β > 90^0, BAT β = 90^0 and BAT β < 90^0) due to constant head variations and variations in rotational speed. This test will also analyze how many rpm the BAT optimum rotation speed results in maximum efficiency. BAT efficiency can be seen from the comparison between the effective power and potential power as shown in equation (4), which results are shown in column 7 of Tables 1-3. Furthermore, the rotational speed and efficiency data are plotted into the curve and the three types of BAT efficiency curves are produced. in Fig. 18-20.

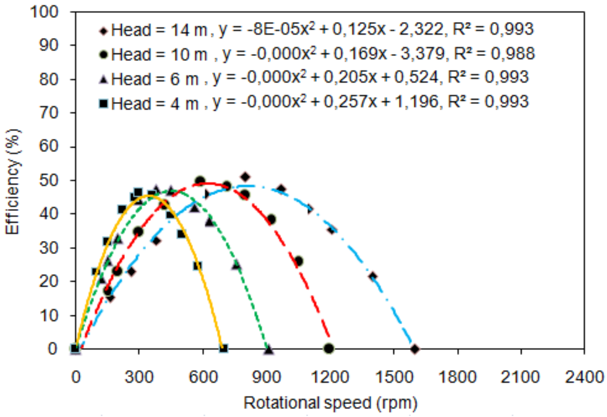

Fig. 18. BAT $\beta < 90^0$ efficiency curve due to the influence of rotation variations

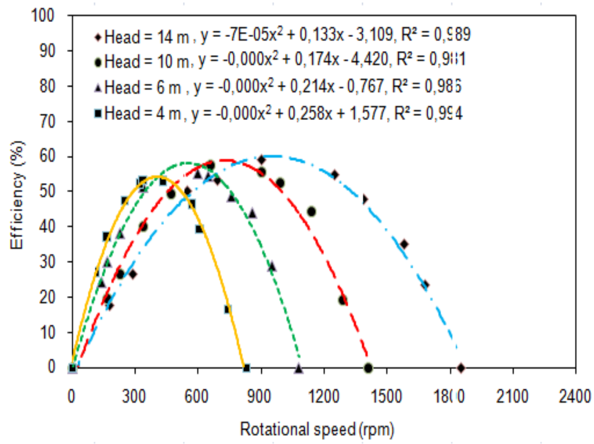

Fig. 19. BAT $\beta = 90^0$ efficiency curve due to the influence of rotation variations

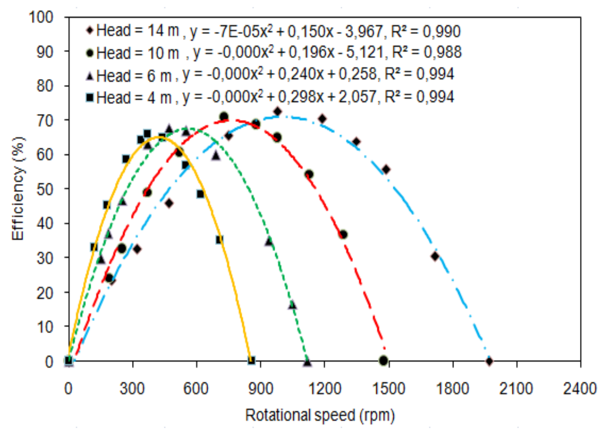

Fig. 20. BAT $\beta > 90^0$ efficiency curve due to the influence of rotation variations

Fig.18-20 show the trend of the efficiency curve to produce a parabolic curve with a quadratic equation with a coefficient of determination (R^2) close to 1.0, which means that changes in efficiency values are balanced with changes in values of rotational speed. The four efficiency curves in each figure have the same pattern, namely in the first half period the efficiency curve tends to increase in the initial rotation speed and in the next half period the efficiency curve continues to decline until it reaches the lowest efficiency. Each curve shows a different trend of increasing efficiency, that is, at a high constant head, the increase in efficiency occurs gradually as seen from the rising and falling trend of the curve. Meanwhile, the lower the constant head value, the increase in efficiency occurs drastically as evidenced by the trend of the curve which goes up steeply and decreases steeply in the next half period of rotation speed. This shows that the lower the constant head, the effect of rotational speed on BAT efficiency will be more limited. Furthermore, the high rotational speed does not represent the optimum rotational speed because the data proves that the highest efficiency is obtained at the rotational speed position at about half the rotation speed period. The size of the modified impeller BAT efficiency curve is larger than the original BAT efficiency curve. This shows that changes in the impeller blade geometry can increase BAT efficiency so that BAT efficiency $\beta > 90^0$ is better than BAT efficiency $\beta = 90^0$ and BAT efficiency $\beta < 90^0$. The maximum efficiency at a constant head of 14 m for BAT $\beta > 90^0$ is 72.8 % occurs at speed optimum rotation of 980 rpm. The next maximum efficiency for BAT $\beta = 90^0$ is 59.1 % at an optimum rotational speed of 900 rpm. The maximum efficiency of BAT $\beta < 90^0$ is 50.9 % at a rotational speed of 800 rpm and a constant head of 14 m. The maximum efficiency reduction of the three types of BAT is around 16.3 %, as the trend is shown in the curve of Fig. 21.

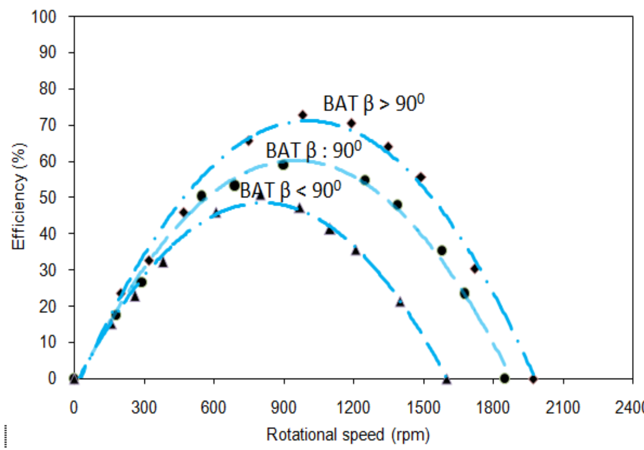

Fig. 21. Maximum efficiency curve of three BAT types

3.4. Effect of Water Flow Variation (Q) on BAT Efficiency (η_b) for Four Constant Head Variations

Discharge is one of the variables that affect BAT performance, so in the following analysis it will be known how the BAT efficiency trend is due to the influence of these discharge variations. Another analysis objective is to determine the starting discharge of each BAT and which BAT is more responsive in generating power. The data in Table 1-3 is interesting to continue to be analyzed, so the discharge and efficiency data as shown in columns 3 and 7 are entered into the curve, and the results are as shown in Fig. 22-24.

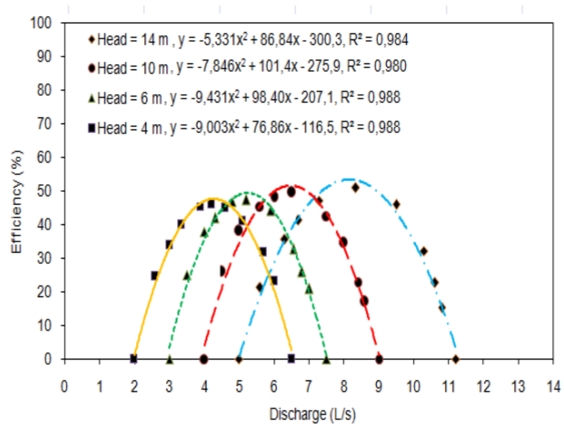

Fig. 22. BAT β > 90^0 efficiency curve due to the influence of discharge variations

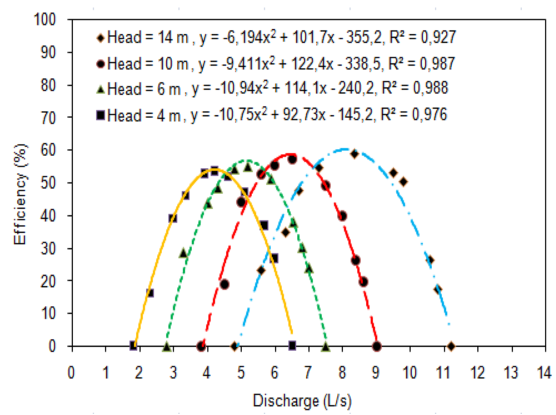

Fig. 23. BAT β = 90^0 efficiency curve due to the influence of discharge variations

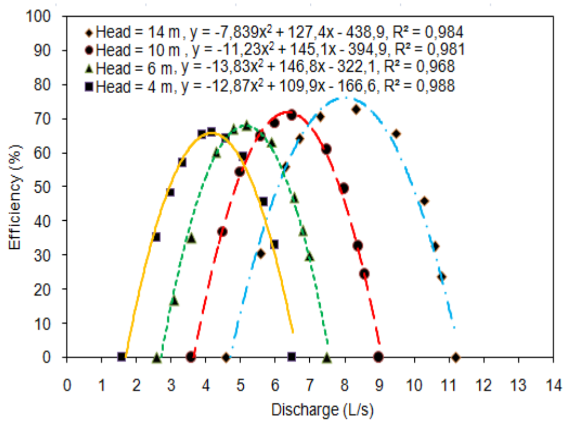

Fig. 24. BAT β < 90^0 efficiency curve due to the influence of discharge variations

Fig. 22-24 shows the BAT efficiency curve due to variations in discharge resulting in a parabolic curve. The four curves have relatively the same trend, only the scales are different. BAT efficiency curve with modified impeller blades has a wider leg size, this shows that changes in the geomery of the impeller blades affect the discharge range that occurs. Another thing that is informed from the curve is that BAT with modified impeller blades produces a smaller starting discharge, this indicates that BAT with modified impeller is more responsive in producing power. There is an inversely proportional relationship between the geometry angle of the BAT impeller blade and the starting discharge. The greater the angle of the impeller blade geometry, the BAT produces a smaller or more responsive starting discharge. The starting discharge for BAT β > 90^0, BAT β = 90^0, and BAT β < 90^0 were 2.0 L/s, 1.8 L/s and 1.6 L/s respectively, there was an increase in the responsiveness of the modified BAT by about 10 %.

3.5. Effect of Discharge Ratio (Q/Q_{max}) on BAT Efficiency (η_b)

The standard curve used by practitioners and observers of turbines as a reference to determine the performance of water turbines is the efficiency curve of five conventional turbines as shown in Fig. 25 [30]. In this curve, there is a trend of Francis turbine efficiency which rises regularly according to the addition of the discharge ratio value. In contrast to pelton turbines and cross flow turbines, the increase in efficiency drastically increases when the discharge ratio is below 0.25 and then the trend of relative efficiency remains even tends to decrease slightly.

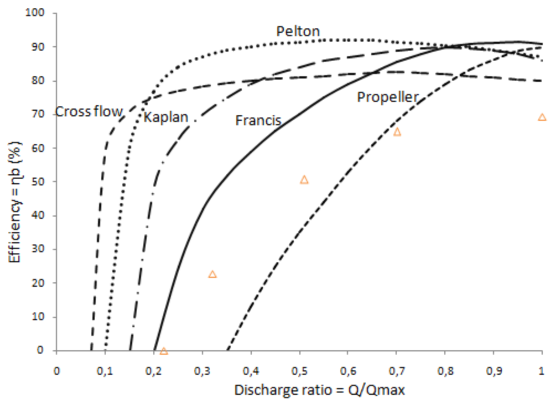

Fig. 25. Conventional turbine efficiency curve

The purpose of this test is to determine the efficiency trend of the three types of BAT due to the influence of variations in the discharge ratio and to compare it with the efficiency trend of five conventional turbines. From testing and analysis of three types of BAT, it was found that there was one value for the rotation speed that produced relatively the same efficiency, namely the rotational speed of 800 rpm. Thus this analysis is focused on the constant rotational speed of 800 rpm with four variations of constant head, namely 4 m, 6 m, 10 m, and 14 m. A summary of the data associated with this analysis is shown in Table 4-6.

Table 4. Data analysis of the effect of the discharge ratio on the efficiency of BAT β < 90^0 or the original BAT

No	*Head*, H (m)	Rotational speed, N (rpm)	Discharge, Q (L/s)	BAT Power, P_b (W)	Discharge ratio, Q/Q_{max}	BAT Efficiency, η_b (%)
1	4	800	_	_	_	_
2	6	800	3.37	37.76	0.41	18.30
3	10	800	5.60	250.34	0.67	45.39
4	14	800	8.34	582.75	1.00	50.90

Table 5. Data analysis of the effect of discharge ratio on BAT efficiency of BAT $\beta = 90^0$

No	*Head*, H (m)	Rotational speed, N (rpm)	Discharge, Q (L/s)	BAT Power, P_b (W)	Discharge ratio, Q/Q_{max}	BAT Efficiency, η_b (%)
1	4	800	2.86	15.96	0.34	14.23
2	6	800	3.52	63.10	0.42	30.45
3	10	800	5.80	31.58	0.69	54.76
4	14	800	8.40	681.77	1.00	59.10

Table 6. Data analysis of the effect of the discharge ratio on the efficiency of BAT $\beta > 90^0$

No	*Head*, H (m)	Rotational speed, N (rpm)	Discharge, Q (L/s)	BAT Power, P_b (W)	Discharge ratio, Q/Q_{max}	BAT Efficiency, η_b (%)
1	4	800	2.73	24.20	0.32	22.80
2	6	800	4.35	130.17	0.51	50.85
3	10	800	5.96	380.05	0.70	65.00
4	14	800	8.52	812.30	1.00	69.42

Futhermore, the discharge ratio and efficiency data in columns 6 and 7 of Table 4-6 are plotted into the curve, and the results are as shown in Fig. 26.

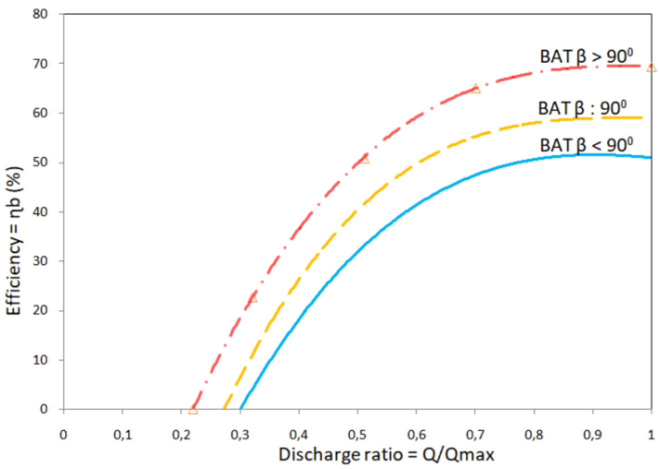

Fig. 26. Efficiency curves of three types of BAT due to the effect of variation in discharge ratio (Q/Q_{max})

The curve in Fig. 26 can be analyzed, that the efficiency trend of the three BATs continues to increase to the maximum efficiency position at the discharge ratio Q/Q_{max} = 1.0. This shows that the three BATs are not saturated but are still reactive in increasing power according to changes in the increase in discharge. The original BAT with the blade shape backwards to the direction of the incoming water of the blade ($\beta < 90^0$) produces a maximum efficiency of 50.9 %. BAT with straight blades or $\beta = 90^0$ and BAT challenging blades or $\beta > 90^0$ resulted in an efficiency of 59.1 % and 69.4 %, an increase in efficiency of 16.11 % and 36.34 %, respectively. The starting discharge ratio is also getting smaller, namely 0.30 compared to 0.27 and 0.22. This shows that BAT $\beta > 90^0$ is more responsive in generating power. This fact is understandable considering that the geometry of BAT $\beta > 90^0$ blades is relatively the same as the geometry of Francis turbine blades. Furthermore, the analysis results show that the efficiency mathematical equations for BAT $\beta > 90^0$, BAT $\beta = 90^0$, and BAT $\beta < 90^0$ are $y = 162.1\ x^3 \neg 479\ x^2 + 473.0\ x \neg 90.39$, R^2 respectively = 0.999, $y = 122.5\ x^3 \neg 385.0\ x^2 + 408.1\ x \neg 72.18$, R^2 = 1,0 and $y = 105.1\ x^3 \neg 363.6\ x^2 + 398.5\ x \neg 89.72$, $R^2 = 1$.

3.6. BAT Efficiency Curves with Conventional Turbines for Comparison

The efficiency curves of the three BAT types are shown in Fig. 26 if plotted in Fig. 25 it will produce a curve as shown in Fig. 27. When compared with the other five conventional turbines, it can be analyzed that the trend and characteristics of each BAT resemble the trend of Francis turbine efficiency, namely increasing regularly according to the addition of the discharge ratio value. Compared to the other four conventional turbines, the Francis turbine has the best performance, with a discharge ratio of 0.9 resulting in an efficiency of about 92%. Observing the curve in Figure 27. it is known that the efficiency of the three BATs is lower than the five conventional turbines, especially the Francis turbine. Furthermore, when compared with the efficiency curve of pump-as-turbine (PAT) [22] and efficiency curve of compressor-as-turbine (CAT) [23], the three BATs are still superior. This is possible because the construction of the BAT volute and impeller is relatively lighter than the PAT and CAT and the change in the BAT blade geometry has a major effect on increasing efficiency. Apart from increasing efficiency, changes to the impeller blade geometry also reduce the discharge ratio. Taking into account this phenomenon, the blade modification BAT defies the direction of water entering the blade (BAT $\beta > 90^0$) is more responsive than the straight blade modified BAT (BAT $\beta = 90^0$), or the blade BAT is backwards towards the direction of water entering the blade or the original impeller blade (BAT $\beta < 90^0$).

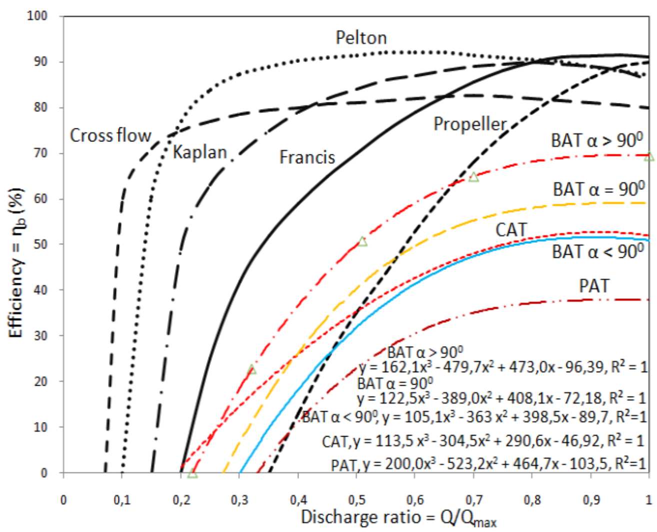

Fig. 27. Efficiency curves for three BAT types versus the efficiency of five conventional turbines

4. Conclusion

The results of the analysis prove that changes in the BAT blade geometry have a positive effect on increasing efficiency. At a head of 14 m. the original BAT impeller with the shape of the blade backwards to the direction of the water entering the blade or the geometry of the angle of the water entering the blade $\beta < 90^0$ produces a maximum efficiency of 50.90 %. BAT impeller modification with straight blades or $\beta = 90^0$ produces a maximum efficiency of 59.10 %, a difference of 8.20 % or an increase in efficiency of about 16.11%. While the BAT impeller modified with a blade that challenges the direction of water entering the blade or $\beta > 90^0$ produces a maximum efficiency of 69.42 %, a difference of 18.52 % from 50.90 % or an increase in efficiency of about 36.38 %. In addition to an increase in efficiency, changes in the shape of the impeller blade also reduce the discharge ratio or can reduce the starting discharge, thus BAT with the impeller blade challenges the direction of water entering the blade or $\beta > 90^0$ is more responsive than the BAT blade straight or $\beta = 90^0$ or the blade backs up to the direction of the water. enter the blade or $\beta < 90^0$. This research has not been completed, further research is needed to determine the optimum angle of water into the blade (β) which can produce maximum efficiency.

Acknowledgements

The success of testing the blower as a turbine is the contribution of many parties, we would like to thank the assistants of the Fluid Dynamics Laboratory at Andalas University.

References

[1] H. Benbouhenni, "Aplication of Five-Level NPC inverter in DPCANN of Doubly Fed Induction Generator for Wind Power Generation Systems", International Journal of SMART GRID, vol. 3, no. 3, pp. 128-137, 2019.

[2] M. I. Abid, M. S. Khalid, M. Kamran, M. A. Rasheed, M. F. Masood and T. Murtaza, "Design and Optimization of the Micro-Hydro Power System for Remote Areas of Pakistan". International Journal of SMART GRID, vol. 4, no. 3, pp. 125-138, 2020.

[3] H. Benbouhenni, "Application of STA Methods and Modified SVM Strategy in Direct Vector Control System of ASG Integrated to Dual-Rotor Wind Power: Simulation Studies", International Journal of SMART GRID, vol. 5, no. 1, pp. 63-73, 2021

[4] D. Siswantoro, and S. L. Z. Ridho," Is Solar Rooftop Power Still Attractive Amid Decreasing Fuel Prices? The Case of Indonesian Electrical Power", International Journal of SMART GRID, vol. 5, no. 2, pp. 83-87, 2021.

[5] E. Bekiroglu and M. D. Yazar, "Analysis of grid connected wind power system", 2019 IEEE International Conference on Renewable Energy Research and Applications (ICRERA), Brasov, Romania, pp. 868-873, 3 - 6 Nov., 2019.

[6] S. M. Kadri, A. O. Bagré, M. B. Camara, B. Dakyo, and Y. Coulibaly, "Electrical power distribution status in West Africa : assessment and perspective overview", 2019 IEEE International Conference on Renewable Energy Research and Applications (ICRERA), Brasov, Romania, pp. 511-515, 3-6 Nov., 2019.

[7] Y. E. A. Eldahab, N. H. Saad, dan A. Z. F. Bahrami, "Assessing Wind Energy Conversion Systems Based on Newly Developed Wind Turbine Emulator". International Journal of SMART GRID, vol. 4, no. 4, pp. 1694-1704, 2020.

[8] E. S. Jones, H. Gong, and D. M. Ionel, "Optimal combinations of utility level renewable generators for a net zero energy microgrid considering different utility charge rates", 2019 IEEE International Conference on Renewable Energy Research and Applications (ICRERA), Brasov, Romania, pp. 1014-1017, 3-6 Nov. 2019.

[9] H. Benbouhenni, "Direct Vector Control for Doubly Fed Induction Generator–Based Wind Turbine System Using Five-Level NSVM and Two-Level NSVM Technique", International Journal of SMART GRID, vol. 3, no. 1, pp. 26-33, 2019.

[10] M.F. Masood, M. I. Abid, M. S. Khalid, T. Murtaza, M. A. Rasheed, H. U. Rehman, and T. Zahid. "A Novel Solution to Eliminate Frequency Intermittency by Adding Spinning Reserve to the Micro-Hydro Turbine Generator Using Real-Time Control of Induction Motor through AC-DC-AC Power Converters", International Journal of SMART GRID, vol. 4, no. 4, pp. 149-156, 2020.

[11] A. N. Bachtiar, "Pengoperasian kembali ribuan kincir air di Sumatera Barat melalui pengembangan sistem kincir teknologi cross flow", Jurnal Teknik Mesin ITP Padang, vol. 4, pp. 1-7, 2014.

[12] A. N. Bachtiar, A. F. Pohan, R. Ervil, Santosa, I. Berd, and U. G. S. Dinata, "Performance of water wheel knock down system (W2KDS) for rice milling drive**",** International Journal on Advanced Science, Engineering and Information Technology (IJASEIT), vol. 11, no. 3, pp. 907-916, 2021.

[13] H.Benbouhenni, "Neuro-Second Order Sliding Mode Field Oriented Control for DFIG Based Wind Turbine", International Journal of SMART GRID, vol. 2, no. 4, pp. 209-217, 2018.

[14] J. A. S. D. Rio, S. G. Holguin, D. H. Zuluaga, and E. C. Arrieta," Effect of Hydrodynamically Designed Blades on the Efficiency of a Michell-Banki Turbine", International Journal of Renewable Energy Research (IJRER), vol 10, no 3, pp. 1165-1173, 2020.

[15] S. Abderrahim, M. Allouche**, and M. Chaabane" A New Robust Control Strategy for a Wind Energy Conversion System Based on a T-S Fuzzy Model", International Journal of SMART GRID, vol 4, no 2, pp. 88-99, 2020.

[16] A. N. Bachtiar, I. Yusti, A. F. Pohan, Santosa, I. Berd, and U. G. S. Dinata, "Performance of a centrifugal pump as a pico hydro scale turbine", Advances in Applied Sciences, vol. 4, no. 4, pp. 88-96, 2019.

[17] A. N. Bachtiar, A. F. Pohan, Santosa, I. Berd, and U. G. S. Dinata, "Performance on compressor-as-turbine (CAT) pico-hydro scale", International Journal of Renewable Energy Research (IJRER), vol. 9, no. 4, pp. 2073-2081, 2019.

[18] A. N. Bachtiar, A. F. Pohan, I. Yusti, R. Ervil, Santosa, I. Berd, and U. G. S. Dinata, "Effect of head variations on performance four sizes of blowers-as-turbines (BAT)", International Journal of Renewable Energy Research (IJRER), vol. 10, no. 1, pp. 343-353, 2020.

[19] F. Dietzel, Turbinen, Pumpen und Verdichter, 5th ed., Freidberg : Vogel Verlag, Wurzburg, 1980

[20] A. H. Church, Centrifugal Pump and Blowers, 2th ed, New York : Robert E. Krieger Publishing Co. Inc., 1944.

[21] Kikai Kenkyu Ltd., Educational machines and equipment, Instruction Manual with Experimental Text Book.Tokyo. 1990, pp. 1-12.

[22] F.M. White, Fluid Mechanic, 7th ed., New York : Mc Graw-Hill, 2008.

[23] R.S. Khurmi, Machine Design, 5th ed., New Delhi : Eurasia Publishing House (Pvt) Ltd, 1984.

[24] U. Meier and SKAT, Local Experience with Micro-Hydro Technology, vol. 11 no. 1, Swiss : St. Gall University, 1981.

.